0026-895X/92/030423-09$03.00/0

MOLECULAR PHARMACOLOGY, 42:423-431

Gate-Dependent Blockade of Sodium Channels by Phenothiazine Derivatives: Structure-Activity Relationships

V. BOLOTINA,[1] K. R. COURTNEY, and B. KHODOROV

Institute of Experimental Cardiology, Cardiology Research Center, USSR Academy of Medical Sciences, Moscow, 121552, USSR (V.B.), Palo Alto Medical Foundation, Palo Alto, California 94301 (K.R.C.), and Institute of General Pathology, USSR Academy of Medical Sciences, Moscow 121552, USSR (B.K.)

Received July 17, 1991; Accepted June 12, 1992

SUMMARY

Voltage-clamp studies of myelinated nerve fibers that are designed to determine structural criteria regarding selective drug blocking of open and inactive states of the sodium channel are described. A series of phenothiazines were studied. It was shown that two of these drugs (ethmozine and ethacizine, at 5 μM) require open channels for blocking action and the other two (chlorpromazine and chloracizine, at 5 μM) can effectively block inactive channels. A size criterion, which looks at the spanning width at the aromatic end of these molecules, can explain this qualitative difference in drug action. Other important differences in the action of these four drugs are described, including their rates of development of drug block and removal of drug block. Relevant critiques of proposed structure-activity hypotheses are given.

Despite considerable progress over the last 15 years in the study of the gate-dependent blockade of Na^+ currents by LA and related drugs (including antiarrhythmics and anticonvulsants), many questions concerning the mechanisms of their interaction with the Na^+ channel macromolecule are not yet settled (for reviews, see Refs. 1–5). Among them is the salient question of the number and location of blocking sites in the Na^+ channel. Another important question deals with the properties of drugs that determine their preference for blocking open or inactivated Na^+ channel conformations. Also, what is the nature of tonic block? Is it produced by drug interactions with open or inactivated Na^+ channels?

One of the experimental approaches to study these and some other questions is a comparative analysis of structure-activity relations for different types of Na^+ channel blockade by LA and related drugs.

The present work continues our previous investigations in this field (6–10). Fig. 1 shows the chemical structure of four derivatives of phenothiazine used in our voltage-clamp experiments on frog node of Ranvier. Among them are two antiarrhythmic drugs, i.e., ETC and ETM, the well known neuroleptic chlorpromazine CHP, and CHC, which exhibits antianginal properties. The chemical structure of these drugs resembles that of classical LA, i.e., aromatic portion-intermediate chain-terminal amino group. The aromatic portion of all these drugs is represented by the phenothiazine ring. The structures of the two other portions of drug molecules vary.

[1] Present address: Vascular Biology, E-401, University Hospital, Boston University Medical Center, 88 East Newton St., Boston, MA 02118-2393.

Our experiments have shown that all these drugs are able to produce UDB of sodium channels. However the mechanism of its development is different; ETC and ETM produce the UDB due to interaction with open Na^+ channels, whereas CHP and CHC interact preferentially with inactivated Na^+ channels.

There are also certain quantitative distinctions in the characteristics of blocking effects within each aforementioned pair (ETC and ETM or CHP and CHC), suggesting a difference in their affinity for a corresponding channel conformation. To elucidate the origin of these distinctions, we have compared the characteristics of the observed blocking effects with the chemical structures, lipid solubilities, and dimensions of these drugs, as estimated by the use of the ALCHEMY molecular modeling system.

Preliminary results of parts of this study have been published previously (11, 12).

Materials and Methods

Experiments were carried out on single myelinated nerve fibers dissected from the sciatic nerve of *Rana ridibunda*. Membrane currents were recorded from the node of Ranvier by means of the voltage-clamp technique (13, 14). The magnitude of the ionic current (I_{Na}), in nA, was calibrated by assuming that the resistance of the intra-axonal current delivering pathway was 20 MΩ (13). Leakage and capacitive currents were substrated electronically.

Unless otherwise mentioned, both ends of the nerve fiber were cut in 114 mM CsF solution. Diffusion of Cs^+ ions along the axoplasm to the node provided effective blockage of the outward potassium currents.

The control Ringer solution used to superfuse the node contained

ABBREVIATIONS: LA, local anesthetics; ETC, ethacizine; ETM, ethmozine; CHP, chlorpromazine; CHC, chloracizine; UDB, use-dependent block.

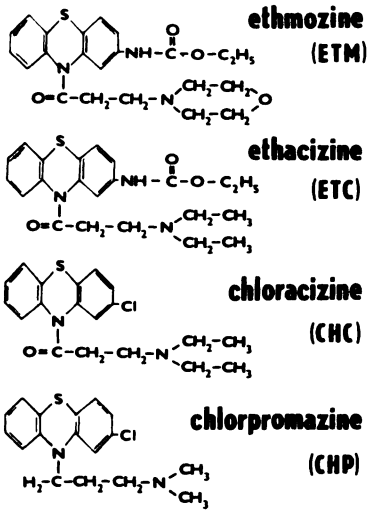

Fig. 1. Chemical structures of the phenothiazine derivatives used, ETM, ETC, CHC, and CHP.

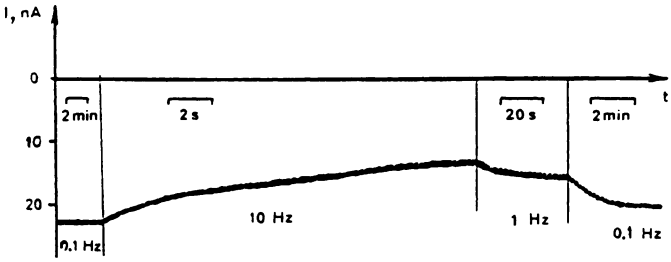

Fig. 2. Modulation of the ETM (5 μM) block by variation of the stimulation frequency in the range of 0.1–10 Hz. The tonic block is not shown. E_h = −90 mV; E_{test} = −10 mV; pulse duration = 10 msec. *Ordinate*, peak I_{Na} value; *abscissa*, duration of the experiment (note different time scales).

(in mM) 114 NaCl, 2.5 KCl, 2.0 $CaCl_2$, and 5 Tris. The pH of all solutions was adjusted to 7.3. Experiments were carried out at 8–12°.

ETM, ETC, CHP, and CHC were added to the external fluid from the corresponding stock solutions just before the experiment. To dissolve these substances two or three drops of ethanol were used; the final concentrations of ETM, ETC, CHP, and CHC in Ringer's solution were 5–25 μM.

Results

Effects of ETC and ETM

Tonic block. When applied to the resting node of Ranvier (E_h = −90 mV), 5 μM ETM produced tonic block, as indicated by a 15–20% decrease in the peak I_{Na} elicited by the first depolarizing test pulse after a period of 5–10 min quiescence (see Fig. 3).

In contrast to ETM, ETC at a concentration of 5 μM failed to produce such tonic block (10 experiments); I_{Na} elicited by the first test pulse applied 10 min after the beginning of ETC treatment was always of the same amplitude as the control current measured before ETC application (see Fig. 5).

Use-dependent (phasic) block. Repetitive stimulation of the nodal membrane treated with 5 μM ETM or ETC led to a pulse by pulse decrease in the peak value of I_{Na}. This is so-called cumulative block or UDB of Na^+ currents.

Fig. 2 illustrates the frequency (f) dependence and the reversibility of the UDB produced by 5 μM ETM after development of the tonic block. It is seen that at f = 0.1 Hz the UDB

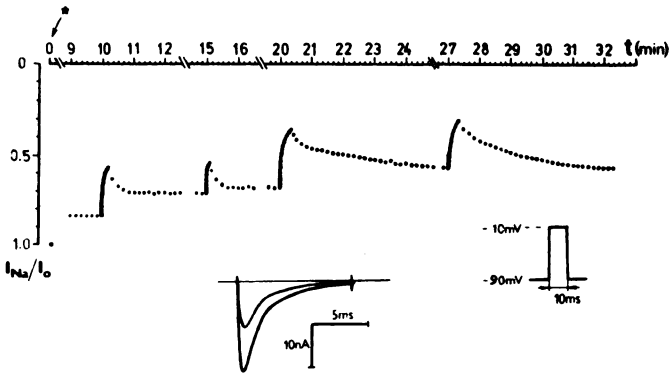

Fig. 3. Effect of repetitive stimulation on the development of Na^+ current blockade by ETM. *Abscissa*, duration of the experiment. Zero corresponds to the moment of ETM application to the membrane (☆). The breaks on the time scale show the periods when test pulsing was stopped (resting membrane conditions). *Ordinate*, relative value of the peak Na^+ currents. I_o, control I_{Na} before ETM application. First point on the graph (at t = 0) corresponds to the peak value of I_{Na} just before ETM application to the membrane. For 9 min after the beginning of ETM (5 μM) treatment, the membrane was held at E_h = −90 mV, without being subjected to stimulation. Test pulses (*inset*) at low frequency (0.1 Hz), started after 9 min of treatment of the resting node by ETM, revealed the stable decrease in I_{Na} that corresponded to the initial tonic block. UDB of I_{Na} was induced by four consecutive trains of test pulses (10 Hz) started at t = 10, 15, 20, and 27 min. The time of high frequency (10 Hz) stimulation was 10, 5, 20, and 20 sec, respectively. The recovery of I_{Na} from the UDB was followed by test pulses at low (0.1 Hz) frequency. The incomplete recovery of I_{Na} from UDB is considered an indication of the development of secondary tonic block.

was absent; at f = 10 Hz we observed a gradual pulse by pulse decrease in I_{Na}. This effect, however, proved to be reversible; a decrease in f first to 1, and then to 0.1 Hz led to a progressive increase in I_{Na}. The latter, however, did not recover to its initial value. Such an incomplete recovery of I_{Na} after termination of repetitive pulsing was also observed in the other experiments with ETM.

An especially notable experiment illustrating this effect is presented in Fig. 3. In this experiment, 9 min after application of 5 μM ETM, when the tonic block reached its saturated value, we applied repetitive stimulation at f = 10 Hz. In 10 sec, I_{Na} decreased to 57% of its initial value. A subsequent decrease in f to 0.1 Hz led to a partial recovery of I_{Na}; I_{Na} reached a new steady state value with time cource of recovery, τ_{fast}, of 16 sec. The next short (5-sec) repetitive pulsing did not affect either the time course of I_{Na} recovery (τ_{fast} = 14 sec) or its steady state poststimulatory value. In contrast, the next 20-sec train of depolarizing pulses induced a more profound decrease in I_{Na} and the appearance of a slow component of I_{Na} recovery (τ_{slow} = 100 sec). I_{Na} reached a new poststimulatory level. This additional stationary block, revealed only after the termination of repetitive pulsing, was labeled conventionally as the secondary or poststimulatory tonic block, in contrast to the ordinary initial tonic block observed during application of a drug to the resting membrane. After I_{Na} reached its new, lower, poststimulatory level, high frequency (10 Hz) repetitive stimulation started to be fully reversible.

After the development of both initial and secondary components of tonic block, peak I_{Na} was stably reduced to 55% of its original value (mean of 15 experiments).

Current-voltage relations (I-E) and the steady state inactivation (h_∞-E), measured before and after development of initial and secondary tonic block, are presented in Fig. 4. The voltage

dependence of activation, and of inactivation, and the I_{Na} reversal potential did not change under these conditions.

The UDB produced by 5 μM ETC is shown in Fig. 5. Although 10-min treatment of the resting node by this concentration of ETC did not produce tonic block, application of the repetitive pulsing immediately caused a gradual decrease in I_{Na}. It is important to note that this cumulative block appeared at frequencies as low as 0.1 Hz, where no signs of UDB could be revealed in the presence of 5 μM ETM. A subsequent increase in f to 0.2 and then to 0.5 and 1 Hz led to a progressive fall of I_{Na} to about 14% of its original value. This UDB proved to be very stable. A decrease in f from 1 to 0.5 and to 0.1 Hz did not lead to recovery of suppressed I_{Na}; it remained practically unchanged.

The current-voltage relations and steady state inactivation measured before and immediately after the termination of repetitive stimulation are presented in Fig. 6. It can be seen that UDB blockade of about 85% of Na^+ channels did not affect either the voltage dependence of activation and inactivation or the current reversal potential.

It will be shown below that a partial recovery of I_{Na} from UDB produced by ETC can be achieved only by application of a hyperpolarizing prepulse before each depolarizing test pulse in a train.

Activation versus inactivation block. As distinct from repetitive pulsing, a single, long-lasting, depolarizing step did not enhance the blocking action of either ETM or ETC. Fig. 7 illustrates the result of one such experiment with ETM and ETC. It is seen that a 2-sec conditioning step from $E_h = -90$ mV to $E_c = -50$ mV caused only fast inactivation of Na^+ channels, as manifested by a 70% reduction in peak I_{Na} level elicited by the test pulse applied immediately after the end of a conditioning depolarization. However, after a 100-msec inter-

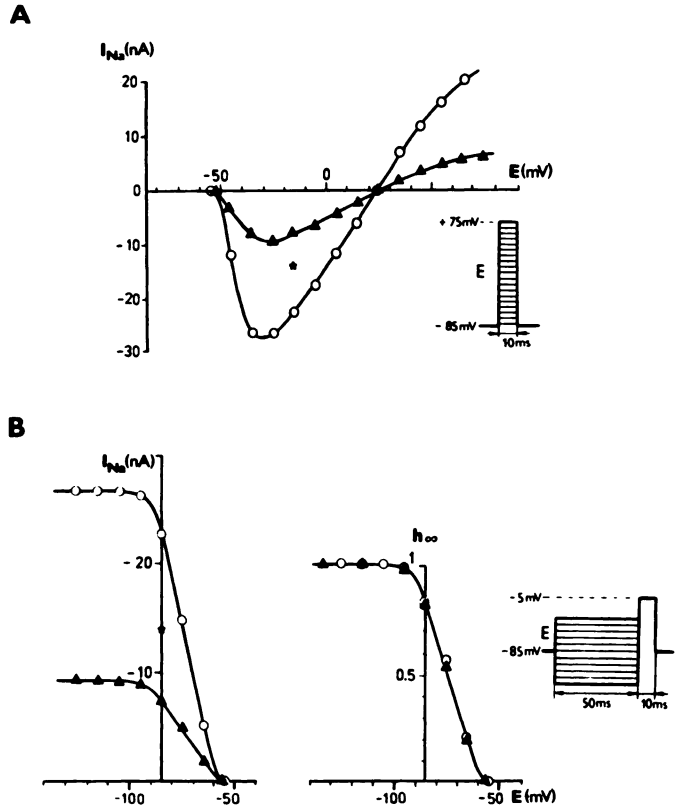

Fig. 4. Effect of ETM on current-voltage relation (A) and steady state fast inactivation curve (B) of Na^+ currents. ○, Before ETM application; ▲, after the development of initial and secondary tonic block in the presence of 5 μM ETM. ☆, Value of I_{Na} after the development of initial tonic block. A, Current-voltage relations. *Abscissa*, membrane potential (E) during the test pulse; *ordinate*, I_{Na}. *Inset*, test pulse parameters. B, Steady state fast inactivation of I_{Na}. *Abscissa in left and right*, membrane potential (E) during a 50-msec prepulse; *ordinate, left*, amplitude of I_{Na} elicited by the test pulse; *right*, normalized values of I_{Na}. *Inset*, pulse program.

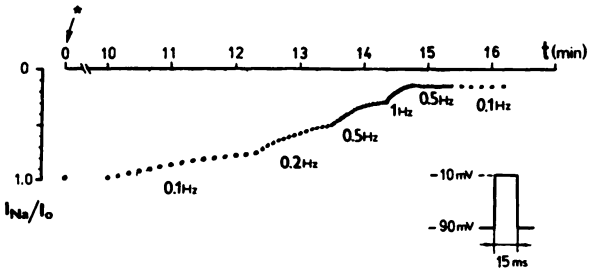

Fig. 5. Development of the stable UDB of I_{Na} by 5 μM ETC. *Ordinate*, relative value of the peak Na^+ currents. I_o, control I_{Na} before ETC application. *Abscissa*, duration of the experiment. Zero corresponds to the moment of ETC application to the membrane (☆). During the first 10 min of ETC treatment, the membrane was held at $E_h = -90$ mV without being subjected to stimulation. From $t = 10$ min, UDB was induced by repetitive pulses (parameters are shown in the *inset*) at different frequencies from 0.1 to 1 Hz and back to 0.1 Hz. See text for details.

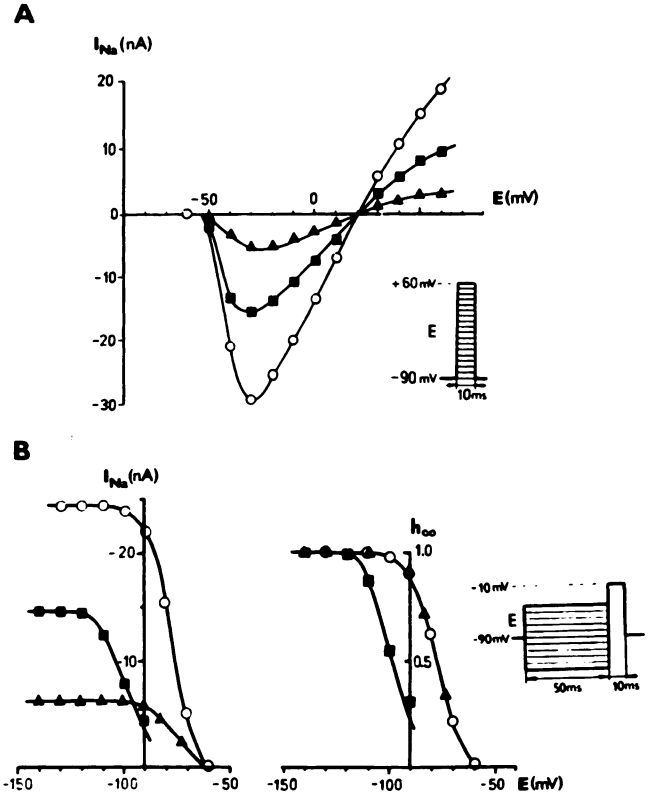

Fig. 6. Effect of ETC on current-voltage relation (A) and steady state fast inactivation curve (B) of Na^+ currents. ○, Before ETC application; ▲, in the presence of ETC after UDB of I_{Na} had reached its steady state level after membrane stimulation; ■, measured after a maximal recovery of I_{Na} from the UDB, with the help of hyperpolarizing prepulses (see Fig. 11). A, Current-voltage relations. *Abscissa*, membrane potential (E) during the test pulse; *ordinate* I_{Na}. *Inset*, test pulse parameters. B, Steady state fast inactivation of I_{Na}. *Abscissa in left and right*, membrane potential (E) during a 50-msec prepulse; *ordinate, left*, amplitude of I_{Na} elicited by the test pulse; *right*, normalized values of I_{Na}. *Inset*, pulse program.

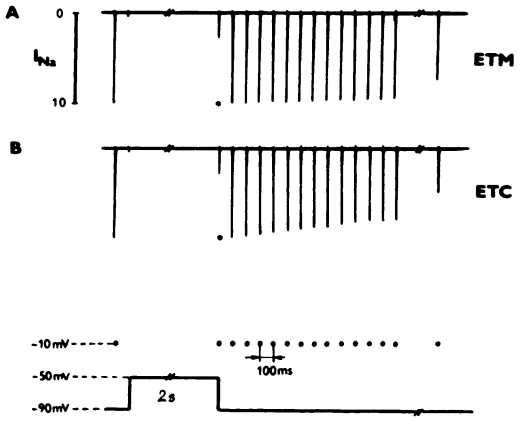

Fig. 7. Comparison of the effects of a single long-lasting depolarization and repetitive membrane stimulation by short pulses on I_{Na} in the presence of 5 μM ETM (A) or ETC (B). Peak Na^+ currents evoked by test pulses are shown in relative values. I_o corresponds to the value of I_{Na} before 2-sec membrane depolarization. *Bottom*, pulse program.

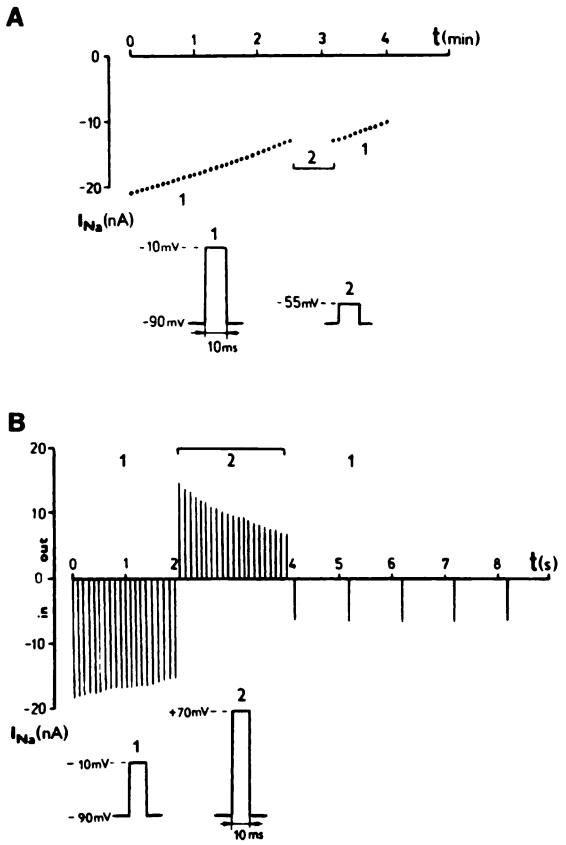

Fig. 8. Effect of subthreshold depolarizing pulses (A) and superthreshold pulses of high amplitude (B) on UDB of Na^+ currents in the presence of ETC (5 μM). A, Inability of subthreshold depolarizing pulses to induce UDB of Na^+ currents. *Ordinate*, I_{Na}; *abscissa*, duration of membrane stimulation with test pulses of different amplitude (pulse programs are shown in *insets*) at the frequency of 0.2 Hz. B, Acceleration of the ETC-induced UDB by strong depolarizing pulses. *Ordinate*, I_{Na}; *abscissa*, time course of stimulation. *Insets*, pulse programs. Subsequent repetitive membrane stimulation (10 Hz) with test pulses to −10 mV (*1*) produced the development of UDB. Increase in pulse amplitude up to +70 mV (*2*) accelerated greatly the cumulative decrease in outward I_{Na}. The block that resulted from this stimulation proved to be very stable after the return of test pulses to −10 mV (*1*), applied at low (1 Hz) frequency.

val a complete recovery of I_{Na} occurred, indicating an inability of ETC to interact with inactivated Na^+ channels. In contrast to a steady state depolarization, the subsequent repetitive (10 Hz) stimulation by 15-msec depolarizing pulses (10 Hz) produced a clear-cut UDB. Qualitatively similar results were obtained in analogous experiments with ETM.

We conclude that ETM and ETC do not block inactivated channels and UDB results from drug interaction with Na^+ channels during their activation.

It is established at present that Na^+ channel activation is a multistep process, culminating in channel opening. To elucidate whether this last step of activation is a prerequisite for development of UDB by ETC, the following pulse procedure was used. The node of Ranvier treated with 5 μM ETC was repetitively stimulated by 15-msec depolarizing pulses, at a frequency of 0.2 Hz (Fig. 8A). At the beginning (during the first 3 min of stimulation), the magnitude of depolarizing pulses (E_t = −10 mV) was large enough to open all the Na^+ channels. This produced a progressive decrease in I_{Na} value (pulse program 1). During the next 0.5 min (pulse program 2), E_t was reduced to a "subthreshold" value of −60 mV. This immediately stopped a further fall of I_{Na}. The block development, however, was resumed as soon as E_t was increased to its initial superthreshold value of −10 mV (pulse program 1). Similar observations were made in analogous experiments with ETM (data not shown). Thus, we conclude that ETC and ETM produced the UDB due to interaction with open Na^+ channels.

The ETC-induced open channel block exhibited a strong voltage dependence, not only in the subthreshold but also in the superthreshold range. Fig. 8B shows that a temporary increase in E_t from −10 to +70 mV in the course of repetitive stimulation greatly enhanced the UDB. So, during the first 2 sec of repetitive pulsing with E_t = −10 mV the inward I_{Na} fell by only 15% from its initial value, whereas during the next 2-sec repetitive stimulation with E_t = +70 mV the outward I_{Na} decreased by about 55%. The UDB enhanced by such high-amplitude membrane stimulation proved to be very stable; after a decrease in E_t to its initial value (E_t of −10 mV), combined with a reduction of frequency to 1 Hz, no recovery of I_{Na} from the block occurred.

In the case of ETM action, an increase in the magnitude of depolarizing pulses from E_t = −10 mV to +70 mV also accelerated and enhanced the UDB. This effect was, however, reversible (in contrast to that observed in experiments with ETC); after a return of E_t to −10 mV, a partial recovery of I_{Na} was observed, which was enhanced by a decrease in the stimulation frequency from 10 to 1 and then to 0.1 Hz (data not shown).

Reversal of UDB by hyperpolarizing prepulses. A stable UDB of Na^+ channels by ETC cannot be attenuated by a single long-lasting (2 sec) hyperpolarizing prepulse (data not shown). In contrast, application of a 50-msec hyperpolarizing prepulses before each test pulse in a train resulted in a gradual recovery of I_{Na}. This restorative effect of prepulses depends on the magnitude of both hyperpolarizing prepulses (E_{pp}) and depolarizing test pulses (E_t) (eight experiments). Fig. 9A clearly shows that I_{Na} recovery occurred only in those cases in which the amplitude of E_t after each hyperpolarizing prepulse was strong enough to open Na^+ channels (pulse program 3). Subthreshold test pulses failed to unblock Na^+ channels after prepulse hyperpolarization (pulse program 2).

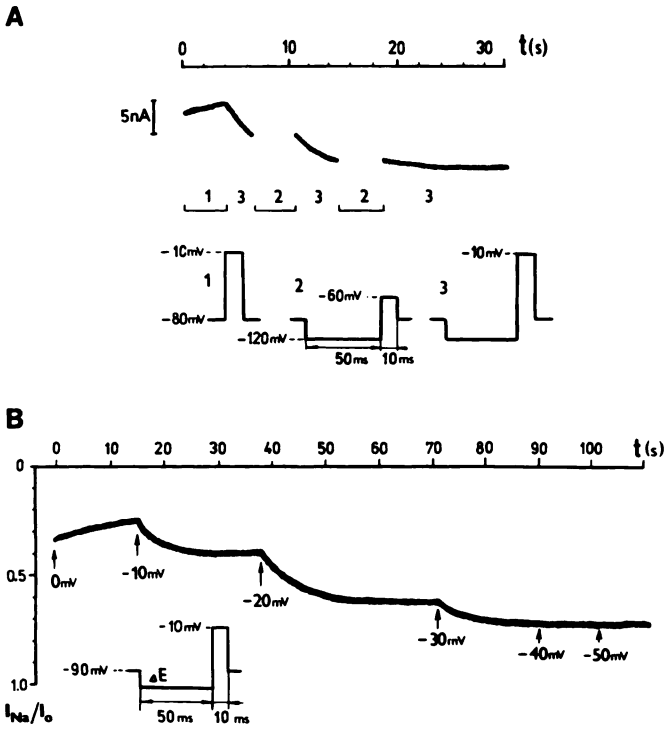

Fig. 9. Restorative effects of hyperpolarizing prepulses on I_{Na} during high frequency (10 Hz) membrane stimulation in the presence of 5 μM ETC. A, Dependence of the restorative effect of hyperpolarizing prepulses on the magnitude of depolarizing test pulses, E_t. *Abscissa*, time course of stimulation; *ordinate*, I_{Na}. *Bottom*, test pulse programs. The UDB of I_{Na} was caused by repetitive (10 Hz) membrane stimulation with test pulses (pulse program 1). Only the final stage of this UDB is shown. When pulse program 1 was replaced by program 3, where a hyperpolarizing prepulse precedes each test pulse, the gradual recovery of I_{Na} was observed. This process, however, was immediately stopped after a decrease in test pulse magnitude to the subthreshold level (pulse program 2). Returning to pulse program 3 led to a resumption in gradual increase of I_{Na}. B, Restorative effect of hyperpolarizing prepulses of different magnitudes on I_{Na}. *Abscissa*, duration of stimulation; *ordinate*, relative value of I_{Na} I_o, peak Na^+ current amplitude before the development of UDB. *Inset*, pulse program. I_{Na} was previously suppressed during the development of UDB by membrane stimulation with test pulses without prepulses (E = 0). Only the final stage of UDB is presented.

A dependence of I_{Na} recovery from UDB on the magnitude of a hyperpolarizing prepulse is shown in Fig. 9B. It can be seen that the extent of I_{Na} recovery increases with an increase in prepulse hyperpolarization up to a certain limit; the maximal increase in I_{Na} was obtained at E_{pp} = −40 mV (i.e., at E_h = −130 mV) and a further increase in E_{pp} failed to enhance unblocking. The *I-E* relation measured at this level of ETC block is shown in Fig. 6A. In Fig. 6B, steady state voltage dependence of I_{Na} recovery is compared with the steady state fast inactivation of I_{Na} (h_∞-E relation) measured before ETC treatment and after saturation of the UDB. In Fig. 6A the absolute values of I_{Na} are plotted, whereas in Fig. 6B the I_{Na} values are normalized to their maximum levels. Fig. 6A shows that even at very negative potential (E = −140 mV), the recovery of I_{Na} from the UDB was only partial; I_{Na} increased to only 60% of its original value (maximal recovery from the secondary tonic block). After normalization of their maxima, curves 1 and 2 (Fig. 6B) coincided, indicating that ETC block did not affect the h_∞-E relation in the population of nonblocked channels. In contrast, curve 3 proved to be shifted to the left by about 20 mV, supporting the view that h_∞-E relations in the population of open-blocked channels are displaced towards hyperpolarization (15, 16).

The effect of hyperpolarizing prepulses on the development of UDB caused by ETM was examined in three experiments. In two of them, the restorative effect of these prepulses was pronounced (data not shown).

Factors that determine frequency dependence of ETM and ETC blockade of Na^+ currents. By using the procedure of unblocking channels with hyperpolarizing prepulses, as described above, it was possible to reveal factors that determine the frequency dependence of ETC- and ETM-induced UDB.

It is known that an enhancement of UDB with stimulation frequency may be determined by two factors, (i) an increase in the number (N) of pulses during a given time interval and (ii) a corresponding reduction of the duration of resting interpulse intervals. To reveal a relative contribution of these two factors to the UDB caused by ETC, we have plotted the dependence of I_{Na} on the number of test pulse (Fig. 10A) at three frequencies, 0.1, 1, and 10 Hz. In the case of ETC action, the I_{Na}-N curves for these three frequency values nearly coincided, indicating that the rate and extent of the ETC block at different resting intervals were determined only by the number of pulses. This implies that, within the range from 0.1 to 10 sec, almost no channels unblock from ETC. This conclusion was supported

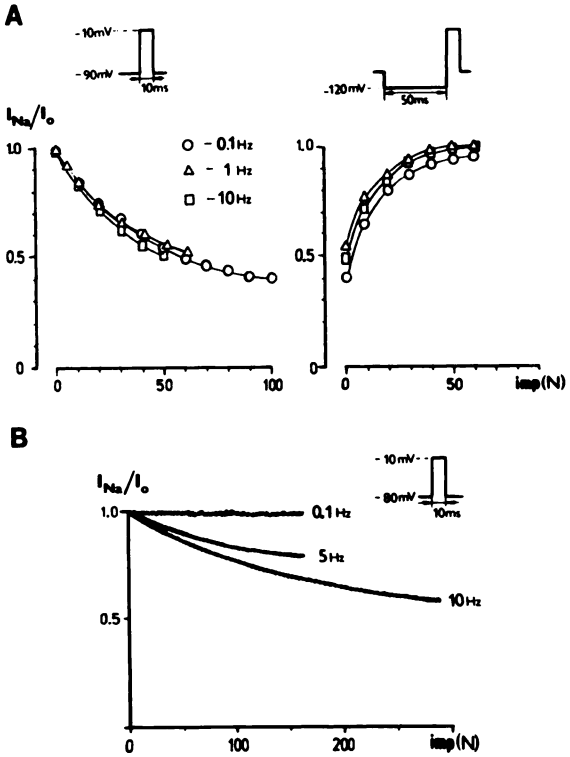

Fig. 10. Dependence of UDB on the frequency of membrane stimulation in the presence of ETC (A) and ETM (B). A, Dependence of I_{Na} on the number (N) of test pulses applied to the membrane with different frequencies (O, 0.1 Hz; Δ, 1 Hz; □, 10 Hz), in the presence of ETC. *Left*, pulse by pulse decrease in I_{Na} during repetitive membrane stimulation with test pulses (*inset*) at frequencies of 0.1, 1, and 10 Hz. *Right*, pulse by pulse restoration of I_{Na} caused by hyperpolarizing prepulses applied before each test pulse (see pulse program in the *inset*). *Abscissa*, number of pulses, *N*; *ordinate*, relative value of I_{Na}. I_o, I_{Na} elicited by the first test pulse in each train. B, Dependence of I_{Na} on the number (N) of test pulses applied to the membrane with the frequency of 0.1, 5, and 10 Hz, in the presence of ETM. *Abscissa*, number of pulses, *N*; *ordinate*, relative value of I_{Na}. I_o, I_{Na} elicited by the first test pulse in each train.

by the fact that the rate and extent of recovery from UDB after the termination of repetitive pulsing also were determined only by the number of "reversal pulses" (a prepulse hyperpolarization followed by test pulse depolarization). Indeed, at the three frequencies used (0.1, 1, and 10 Hz) the recovery from UDB proceeded at nearly the same rate (Fig. 10B).

The UDB induced by ETM, in contrast to that produced by ETC, depends on both N and interpulse intervals, as follows from Fig. 10B; after the same number of pulses, the block was deeper at $f = 10$ Hz than at $f = 5$ Hz. At $f = 0.1$ Hz, the ETM-induced UDB was absent. This evidently means that ETM, in contrast to ETC, is able to escape from the blocked channel not only during application of a depolarizing pulse but also during the resting interpulse intervals.

Effects of CHP and CHC

Application of 5 μM CHP to the resting node of Ranvier did not produce tonic block (five experiments). This is illustrated in Fig. 11, where peak I_{Na} measured 10 min after the beginning of CHP treatment did not differ from that before CHP application. Repetitive stimulation at $f = 0.1$ Hz also failed to induce a reduction of I_{Na}. However, an increase in f to 1 Hz and then to 10 Hz induced a clear cut frequency-dependent inhibition of I_{Na}. This UDB proved to be readily reversible; a decrease in f to 1 and to 0.1 Hz caused a gradual recovery of I_{Na} to its original value, showing no secondary tonic block in the presence of CHP.

Like CHP, CHC at a concentration of 5 μM did not produce tonic block (data not shown). Repetitive stimulation of the nodal membrane treated with CHC induced UDB of I_{Na}, which, however, was much weaker than that induced by 5 μM CHP.

In order to elucidate the nature of this UDB, we have compared the aforementioned effect of repetitive membrane depolarization by short pulses with that produced by a single, long-lasting, conditioning depolarization.

Fig. 12 presents the result of such an experiment with CHP and CHC. It is seen that a 2-sec depolarizing step from −110 to −50 mV caused a considerable decrease in I_{Na} and that recovery from this block proceeded very slowly after termination of this depolarization. The time constants of this recovery in these experiments were 950 msec and 1.5 sec for CHP and CHC, respectively. Qualitatively similar results were obtained in other experiments with CHP and CHC; in all the cases, a prolonged membrane depolarization greatly enhanced the

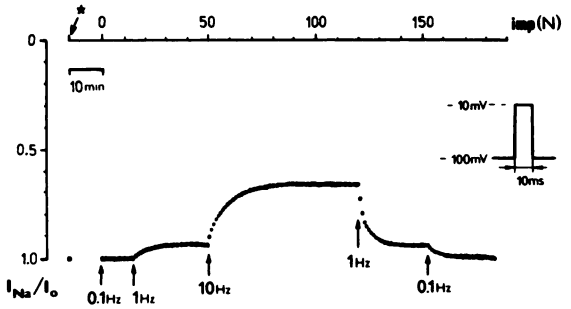

Fig. 11. Modulation of CHP UDB by variation in the frequency of repetitive stimulation. *Ordinate*, relative value of peak I_{Na}. I_o, control value of I_{Na} before CHP application. *Abscissa*, number of pulses, N. CHP (5 μM) was applied to the membrane at the moment shown (☆). No pulses were applied to the membrane during the first 10 min of CHP treatment. Repetitive stimulation was then applied, with test pulses (*inset*) applied at different frequencies, as shown. See text for details.

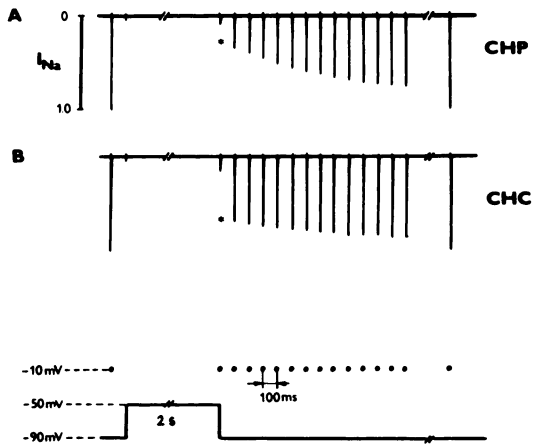

Fig. 12. Slow recovery of I_{Na} after a single prolonged (2 sec) membrane depolarization in the presence of 5 μM CHP or CHC. Peak Na^+ currents evoked by test pulses are shown in relative values. I_{Na} magnitude before 2-sec membrane depolarization was taken as 1.0. *Bottom*, pulse program. I_{Na} recovery after the end of a conditioning depolarization proceeded with time constants of 950 msec for CHP and 1.5 sec for CHC.

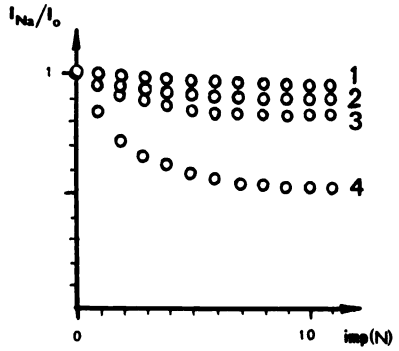

Fig. 13. Dependence of UDB caused by CHP on the duration of depolarizing pulses at a constant frequency of stimulation (10 Hz). *Curves 1, 2, 3,* and *4*, pulse durations of 1, 5, 10, and 50 msec, respectively. *Abscissa*, number of test pulses, N; *ordinate*, relative value of I_{Na} amplitude. Initial value of I_{Na} elicited by the first stimulus in each train was taken as unity. $E_h = -100$ mV. CHP was applied at a concentration of 5 μM.

blocking action of this compound, producing the slowly reactivatable state, resembling that caused by classical LA. This pattern of I_{Na} recovery is characteristic of the effects of all the blockers interacting with inactivated Na^+ channels, including the classical tertiary amine LA (17–19) and some antiarrhythmic and anticonvulsants drugs (6, 20–22). Conventionally, this process was designated as a "drug-induced slow inactivation" (23).

It is well known that the UDB resulting from interaction of drugs with inactivated Na^+ channels is strongly dependent on pulse duration (19, 24, 25). Such a dependence was also revealed in studying the UDB produced by CHP. Fig. 13 illustrates the effect of increasing of pulse duration from 1 to 50 msec on the UDB produced by repetitive (10 Hz) membrane stimulation. Both the rate and extent of the block increased, indicating once more a preference of CHP for the inactivated channels conformation.

Thus, we can conclude that both CHP and CHC are capable of interacting with inactivated Na^+ channels and that this interaction underlies the UDB produced by these compounds.

Discussion

The results of the present work support the notion of the existence of two types of UDB, resulting from interaction of blocking drugs with either open or inactivated Na^+ channels (5, 19). A detailed analysis of the blocking action of four phenothiazines of similar chemical structure allows us to conclude that two of them (ETC and ETM) belong to the group of open channel blockers, whereas the other two (CHP and CHC) interact preferentially with inactivated Na^+ channels.

Kinetic model for UDB produced by open channel blockers ETC and ETM. The use-dependent inhibition of I_{Na} produced by ETC and ETM during repetitive membrane stimulation can be readily interpreted in the framework of a kinetic scheme (scheme 1) similar to that proposed by Courtney (15) for a description of the analogous effects of the lidocaine derivative GEA 968 on the node of Ranvier. From the experimental data presented in the present study, it is clear that ETC interacts only with the channels in the open state. Indeed, no block of I_{Na} was observed when channels remained in resting state (Fig. 5). Inactivated channels also were not blocked by ETC, as revealed in the experiments with long lasting membrane depolarization (Fig. 7). During the repetitive stimulation, UDB of I_{Na} in the presence of ETC developed only when the magnitude of test pulses was sufficient to open the channels (Fig. 8A).

Thus, the development of UDB in the presence of ETC can be presented in the following way.

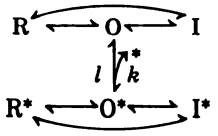

Scheme 1

Here R, O, and I are the resting, open, and inactivated states of unblocked Na^+ channels, R*, O*, and I* are the corresponding states of drug-bound channels, and k and l are the forward and backward rate constants of O-O* transition, with k containing drug concentration as an intrinsic factor.

During each depolarizing pulse, a certain fraction of open channels (O) interact with an ETC molecule (*) and transit first to the "open-blocked" state O* and then to the inactivated-blocked state I*. The other unblocked channels undergo normal activation-inactivation transitions (R→O→I or R→I). At the end of each depolarizing pulse (returning to the initial E_h = −90 mV), these unblocked channels undergo reactivation via the I→R pathway. In contrast, most blocked channels remain in the I* state, due to a negative shift in the voltage dependence of their inactivation (see Fig. 6). In this respect, the effects of ETC resemble those of some other drugs interacting with open channels [such as GEA 968 (15), QX-314 (27), and yohimbine (27)].

The striking feature of ETC block under the conditions of our experiments was the impossibility of obtaining I_{Na} recovery from UDB at rest after the end of repetitive pulsing (Fig. 5). ETC failed to escape from blocked channels when they were in a resting or inactivated state. To cause partial I_{Na} unblocking from ETC, it was necessary not only to introduce hyperpolarizing prepulses before each depolarizing test pulse in a train (see Fig. 9) but also to apply test pulses of sufficient magnitude to open the channels (see Fig. 9A). This experiment shows that ETC can escape only from the channels in the open state (O*↛O) after their transition from inactivated to resting blocked state (I*→R*). Thus, scheme 1 fully describes ETC interactions with Na^+ channels during UDB of I_{Na}.

The kinetic scheme (scheme 1) can be also used for the formal description of UDB produced by ETM. This drug, however, differs from ETC in its unblocking from the Na^+ channels. This occurs not only during depolarizing pulses (as in the case of ETC) but also at rest during interpulse intervals. The results of experiments presented in Fig. 3 and Fig. 10B support this conclusion.

To describe formally the interaction of CHP or CHC with inactivated Na^+ channels, one can use a simplified model proposed by Khodorov *et al.* (19) for tertiary amine LA.

Scheme 2

A LA-like drug (DSI*) interacts, during prolonged membrane depolarization, with an inactivated Na^+ channel (I) and induces its transition to a new state resembling the normal slow inactivation state, conventionally called the "drug-induced slow inactivation" state (DSI*). Here k is the concentration-dependent forward rate constant and l is the concentration-independent reverse (unblocking) rate constant.

In this model, channel reactivation proceeds only via the DSI*→I→R pathway, where dissociation of the drug-receptor complex both is a prerequisite and is rate-limiting for the reverse-transitions of the channel; the more strongly bound a drug is to its receptor, the smaller is the rate of reactivation.

Hille (16) and Hondeghem and Katzung (28) believed that slow reactivation may proceed via two pathway, one shown in scheme 1 and the other, which includes state R*, shown in scheme 3.

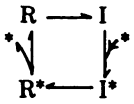

Scheme 3

Here I* = DSI*, as in scheme 2.

The available data are not sufficient to allow a choice between these two models for drugs interacting with inactivated channels.

Structure-activity relationships. At first glance, a preferential interaction of CHP and CHC with inactivated Na^+ channels can be easily explained in the framework of physical interpretation of the modulated receptor hypothesis of Hille (16) and Hondenghem and Katzung (28). Indeed, according to this hypothesis, the route by which a blocking drug can reach its receptor, located in the inner channel mouth, is determined by the lipid solubility of this drug. Lipid-soluble drug forms are thought to come and go from the receptor via hydrophobic regions of the membrane ("hydrophobic pathway"), whereas charged and less lipid-soluble forms go via the hydrophilic pathway (the inner channel mouth).

Table 1 presents the physicochemical characteristics of the drugs used, including pK_a values and calculated partition (P) and distribution (Q) coefficients (octanol/water), which are assumed to reflect the lipid solubility of the drugs. It can be seen that the lipid solubility of CHP and CHC greatly exceeds that of ETC and ETM. Thus, according to the modulated receptor hypothesis, these drugs should use the hydrophobic pathway to the receptor, in contrast to the hydrophilic drugs ETC and ETC, which interact with open Na^+ channels via the

TABLE 1
Physicochemical traits of drugs

	pK_a	logP^a	logQ^b
CHP	9.3	5.3	3.3
CHC	9.0	4.3[c]	2.6
ETC	9.0	1.5[c]	0
ETM	6.3	0.5[c]	0.5

[a] log$P$ is log(partition coefficient) for octanol/water.
[b] Distribution coefficient log$Q$ = log$P$ − log(1 + $10^{pK_a-7.3}$). Neither log$P$ nor pK_a is temperature-adjusted to 10°, so they are intended to provide relative solubilities only.
[c] Estimate based on the measured value for CHP (45) and application of the fragment estimation technique of Hansch and Leo (45).

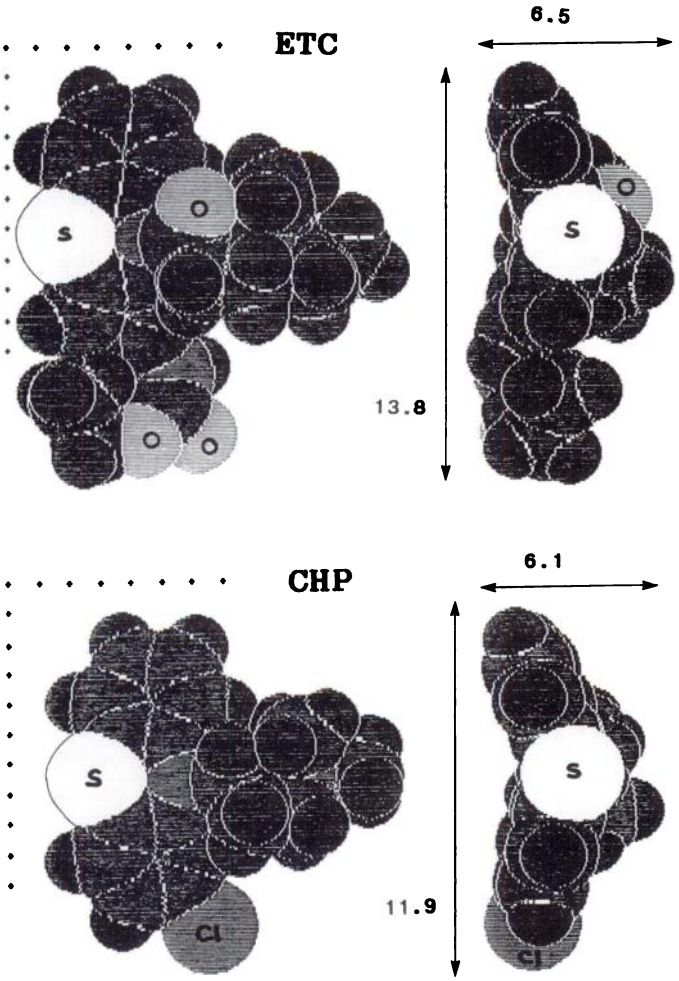

Fig. 14. Dimensions of ETC and CHP, obtained using ALCHEMY molecular modeling software. *Left*, maximally exposed views (1 Å grid); *right*, end-on views, with minimum dimension X and spanning dimension Y_a. The dimensions of ETM are like ETC, and CHC is like CHP.

hydrophilic route. These relations resemble those existing between lidocaine and its tertiary derivative compound GEA 968; lidocaine (log P = 2,4, log Q = 1.7) interacts preferentially with inactivated channels, whereas the highly hydrophilic compound GEA 968 (log P = 1.2, log Q = 0.65) produces UDB of open Na^+ channels (7, 15, 16).

However, many other observations show that lipid solubility is not the only factor determining the preference of a blocking drug for inactivated or open channel conformations. For example, quinidine has a relatively high lipid solubility (log P = 3.6, log Q = 2.56) but interacts preferentially with open Na^+ channels both in nerve fibers (29) and in cardiac cells (30).

Another example is provided by mexiletine. It interacts preferentially with inactivated Na^+ channels in nerve fibers, skeletal muscles (31), and cardiac cells (31, 32). However the lipid solubility of mexiletine is lower than that of ETC (log P = 1.3, log Q = −0.5 at pH 7.3).

This motivated a search for other factors that may determine drug preference for blocking open or inactivated channels. Recently, Courtney (10) has advanced a hypothesis, according to which the specific dimensions of blocking drugs play a decisive role in the choice of the pathway to the channel receptor.

This new size hypothesis uses the spanning dimension at the aromatic end of the molecule in order to explain whether a drug requires open channels in order to exert its blocking effect (10, 11, 33). Fig. 14 depicts the analysis of ETC and CHP dimensions using the ALCHEMY molecular modeling software. Both ETC (Fig. 14A) and ETM (not shown) have dimension Y_a = 13.8 Å and interact only with open channels. Two other drugs, CHP (Fig. 14B) and CHC (not shown), have a smaller Y_a, of 11.9 Å, and are able to block inactivated channels. The dimension Y_a clearly distinguish between these two drug pairs.

There are a few failures of the Y_a dimension hypothesis, all compounds having small Y_a dimension but still requiring open channels to block (15, 34, 35). It appears that extremely poor lipid solubility of some drugs can provide important exceptions to this size rule. But, as long as drugs are relatively "trim" at the tertiary nitrogen end of the molecule and have good lipid solubility, the Y_a hypothesis appears to hold.

Although the Y_a dimension may determine the preferential interaction of ETC and ETM with open Na^+ channels, some other property of these drugs should define the differences in rates of I_{Na} recovery from UDB produced by these compounds. We have seen that ETC, in contrast to ETM, is essentially unable to escape from the blocked channels during 10-sec interpulse intervals (see Fig. 5). This results in the development of UDB during low frequency (0.1 Hz) membrane stimulation (see Fig. 5) and in the dependence of UDB only on the number of test pulses and not on the interpulse intervals (see Fig. 10A). Meanwhile, the only discernible difference between the chemical structures of ETC and ETM concerns their terminal amino groups, i.e., a diethylamino group in ETC and a morpholino group in ETM (see Fig. 1). It is clear that the protonated diethylamino group can provide both electrostatic and hydrophobic interactions with the channel receptor; the positively charged nitrogen can bind to the anionic site of this receptor, whereas the diethyl-alkyl termini of the amino group are able to interact hydrophobically with nonpolar regions of the inner channel wall near the anionic site. In contrast, the oxygen-containing morpholino group of ETM is characterized by a lower hydrophobicity (and much reduced pK_a), which may hinder its binding to the channel receptor. This suggestion is supported by the existing data on the role of hydrophobic interactions of amino groups with the binding sites in Na^+ (26, 36) or K^+ (37) channels.

Comparison with the published data on effects of phenothiazine derivatives on cardiac Na^+ channels. In cardiac cells as well as in nerve fibers (see above), CHP interacts preferentially with inactivated Na^+ channels (38). The situation for ETM and ETC is more complicated. In contrast to that we have seen in experiments with nerve fibers, in cardiac cells ETC (39) and ETM (32, 40) are able to interact with both open

and inactivated Na^+ channels. Thus, once more we can see that cardiac and nerve fiber Na^+ channels differ in their pharmacological properties (41–44).

References

1. Strichartz, G. R., and J. M. Ritchie. The action of local anesthetics on ion channels in excitable tissues. *Handb. Exp. Pharmacol.* **81**:21–51 (1987).
2. Courtney, K. R., and G. R. Strichartz. Structural elements which determine local anesthetic activity. *Handb. Exp. Pharmacol.* **81**:54–94 (1987).
3. Boutherworth, J., and G. R. Strichartz. Molecular mechanisms of local anesthesics. *Anesthesiology* **72**:711–734 (1990).
4. Hondeghem, L. M., and B. G. Katzung. The modulated receptor mechanism of action of sodium and calcium channel blocking drugs. *Annu. Rev. Pharmacol. Toxicol.* **24**:387–423 (1984).
5. Khodorov, B. Role of inactivation in local anesthetic action. *Ann. N. Y. Acad. Sci.* **625**:224–248 (1991).
6. Khodorov, B. I., and L. Zaborovskaya. Blockage of Na and K channels in the node of Ranvier by ajmaline and *N*-propyl-ajmaline. *Gen. Physiol. Biophys.* **2**:233–268 (1983).
7. Khodorov, B., and L. Zaborovskaya. Use-dependent blockade of sodium channels by local anesthetics and antiarrhythmic drugs: effects of chloramine-T. *Drugs Exp. Clin. Res.* **12**:743–752 (1986).
8. Courtney, K. Inactive versus open channel blocking of cardiac sodium channels. *Biophys. J.* **41**:76 (1983).
9. Courtney, K. Review: quantitative structure/activity relations based on use-dependent block and reprining kinetics in myocardium. *J. Mol. Cell. Cardiol.* **19**:319–330 (1987).
10. Courtney, K. Why do some drugs preferentially block open sodium channels? *J. Mol. Cell. Cardiol.* **20**:461–464 (1988).
11. Bolotina, V., S. Revenko, and B. Khodorov. Stimulus-dependent ethmozin blockade of sodium channels (in Russian). *Neurophysiology.* **13**:380–388 (1981).
12. Bolotina-Simanova, V., and B. Khodorov. Interaction of phenothiazines and phenobarbital with open or inactivated sodium channels in node of Ranvier. *Physiol. Bohemoslov.* **35**:347 (1986).
13. Dodge, F., and B. Frankenhaeuser. Sodium currents in isolated frog nerve fibres under voltage-clamp conditions. *J. Physiol. (Lond.)* **143**:75–90 (1959).
14. Hille, B. The permeability of sodium channel to organic cations in myelinated nerve. *J. Gen. Physiol.* **58**:599–619 (1971).
15. Courtney, K. Mechanisms of frequency-dependent inhibition of sodium currents in frog myelinated nerve by the lidocaine derivative GEA 968. *J. Pharmacol. Exp. Ther.* **195**:225–236 (1975).
16. Hille, B. Local anesthetics: hydrophilic and hydrophobic pathways for the drug-receptor reaction. *J. Gen. Physiol.* **69**:497–515 (1977).
17. Khodorov, B. I., E. Peganov, and L. Shishkova. Slow sodium inactivation in the membrane of the node of Ranvier (in Russian), in *Biophysics of Membranes*, Kaunas, 620–625 (1973).
18. Khodorov, B. I., L. Shishkova, and E. Peganov. Effect of procaine and calcium ions on the slow sodium inactivation in frog node of Ranvier (in Russian). *Bull. Exp. Biol. Med.* **3**:10–14 (1974).
19. Khodorov, B. I., L. Shishkova, E. Peganov, and S. Revenko. Inhibition of sodium currents in frog Ranvier node treated with local anesthetics: role of slow sodium inactivation. *Biochim. Biophys. Acta* **433**:409–435 (1976).
20. Revenko, S., B. Khodorov, and M. Avrutzky. Antiarrhythmic cordaron blocks inactivated sodium channels. *Bull. Exp. Biol. Med.* **7**:702–704 (1980).
21. Courtney, K. R. Slow sodium channel inactivation and the modulated receptor hypothesis: application to phenobarbital. *Biochim. Biophys. Acta* **642**:433–487 (1981).
22. Schwartz, J., B. Brom, and G. Ochs. Phenobarbital induces slow recovery from sodium inactivation at the nodal membrane. *Biochim. Biophys. Acta* **597**:384–390 (1980).
23. Khodorov, B. I. Some aspects of the pharmacology of sodium channels in nerve membrane: process of inactivation. *Biochem. Pharmacol.* **28**:1451–1459 (1979).
24. Chernoff, D., and G. R. Strichartz. Kinetics of local anesthetic inhibition of neuronal sodium currents, pH and hydrophobicity dependence. *Biophys. J.* **58**:69–81 (1990).
25. Gilliam, F. R., C. F. Starmer, and A. O. Grant. Blockade of rabbit atrial sodium channels by lidocaine. *Circ. Res.* **65**:723–739 (1989).
26. Strichartz, G. R. The inhibition of sodium currents in myelinated nerve by quaternary derivatives of lidocaine. *J. Gen. Physiol.* **62**:37–57 (1973).
27. Revenko, S., B. Khodorov, and L. Shapovalova. Quinidine blockade of sodium and potassium channels in myelinated nerve fibre (in Russian). *Neurophysiology* **14**:324–330 (1982).
28. Hondeghem, L. M., and B. G. Katzung. Time- and voltage-dependent interactions of antiarrhythmic drugs with cardiac sodium channels. *Biochim. Biophys. Acta* **472**:373–398 (1977).
29. Revenko, S., B. Khodorov, and L. Shapovalova. The effects of yohimbine on sodium and gating current in frog Ranvier node membrane. *Neuroscience* **7**:1377–1387 (1982).
30. Kodama, I., J. Toyama, C. Takanaka, and K. Yamada. Block of activated and inactivated sodium channels by class-I antiarrhythmic drugs studied by using the maximum upstroke velocity (V_{max}) of action potential in guinea pig cardiac muscles. *J. Mol. Cell. Cardiol.* **19**:367–377 (1987).
31. Courtney, K. Comparative actions of mexiletine on sodium channels in nerve, skeletal and cardiac muscle. *Eur. J. Pharmacol.* **74**:9–18 (1981).
32. Schubert, B., S. Hering, R. Bodewei, L. Rosenstraukh, and W. Wollenberger. Use- and voltage-dependent depression by ethmozine (moricizine) of the rapid inward sodium current in single rat ventricular muscle cells. *J. Cardiovasc. Pharmacol.* **8**:358–366 (1986).
33. Singh, B., and K. Courtney. The classification of antiarrhythmic mechanisms of drug action: experimental and clinical considerations, in *Cardiac Electrophysiology: From Cell to Bedside* (D. Zipes and J. Jalife, eds.). W. B. Saunders, Philadelphia, 882–897 (1990).
34. Kodama, I., H. Honjo, K. Kamiya, and J. Toyama. Two types of sodium channel block by class-I antiarrhythmic drugs studied by using V_{max} of action potential in single ventricular myocytes. *J. Mol. Cell. Cardiol.* **22**:1–12 (1990).
35. Yeh, J., and R. E. Ten Eick. Molecular and structural basis of resting and use-dependent block of sodium currents defined using disopyramide analogs. *Biophys. J.* **51**:123–135 (1987).
36. Yeh, J. A pharmacological approach to the structure of the Na channel in squid axon, in *Protein in the Nervous System: Structure and Function*. 17–49 (1982).
37. Swenson, R. Inactivation of potassium current in squid axon by a variety of quaternary ammonium ions. *J. Gen. Physiol.* **77**:255–271 (1981).
38. Ogata, N., M. Nishimura, and T. Narahashi. Kinetics of chlorpromazine block of sodium channels in single guinea-pig cardiac myocytes. *J. Pharmacol. Exp. Ther.* **243**:605–613 (1989).
39. Wollenberger, W., and B. Schubert. Single heart muscle cells and their reaggregates as models for the study of the action of class I antiarrhythmic drugs on the sodium channel. *J. Cardiovasc. Pharmacol.* 61–72 (1987).
40. Makielski, J., A. Undrovinas, D. Hanck, M. Sheets, V. Nesterenko, L. Alpert, L. Rosenstraukh, and H. Fozzard. Use-dependent block of sodium current by ethmozin in voltage-clamped internally perfused canine cardiac Purkinje cells. *J. Mol. Cell. Cardiol.* **20**:255–265 (1988).
41. Cohen, C., B. Bean, and R. Tsien. Tetrodotoxin block of sodium channels in rabbit Purkinje fibres: interactions between toxin binding and channel gating. *J. Gen. Physiol.* **78**:383–411 (1981).
42. Sokolova, S., Y. Zilberter, and B. Khodorov. Slow inactivation of sodium channels in isolated myocardial cells (in Russian). *Biol. Membr.* **4**:865–874 (1987).
43. Sokolova, S., Y. Zilberter, and B. Khodorov. Gate-dependent interaction of lidocaine and tetrodotoxin with sodium channels in isolated cardiac cells (in Russian). *Biol. Membr.* **5**:932–949 (1988).
44. Zilberter, Y., L. Motin, S. Sokolova, A. Papin, and B. Khodorov. Ca-sensitive slow inactivation and lidocaine-induced block of sodium channels in rat cardiac cells. *J. Mol. Cell. Cardiol.* **23**: (Suppl. 1):61–72 (1991).
45. Hansch, C., and A. Leo. *Substituent Constants for Correlation Analysis in Chemistry and Biology*. Wiley, New York. (1979).

Send reprint requests to: Victoria Bolotina, Vascular Biology, E-401, University Hospital, Boston University Medical Center, 88 East Newton St., Boston, MA 02118–2393.